Degree final thesis
Biochemistry and Molecular Biology

ROLE OF THE MITOCHONDRIAL PROTEIN MCJ IN THE DEVELOPMENT OF NON-ALCOHOLIC FATTY LIVER DISEASE (NAFLD)

Author:
Sofía Lachiondo Ortega

Director:
Dr. Antonio Gómez Muñoz

Co-director:
Dr. Mª Luz Martínez-Chantar

TABLE OF CONTENTS

1. SUMMARY

Non-alcoholic fatty liver disease (NAFLD) is the most common chronic liver disease in Western world, affecting 20-30% of the general population. NAFLD comprises a broad range of clinical disorders from pure steatosis and non-alcoholic steatohepatitis (NASH) to cirrhosis and liver cancer. However, the molecular mechanisms underlying NAFLD progression are not completely understood and the tools for its early diagnosis are limited. Notably, mitochondrial alterations have been described in a variety of chronic liver diseases, including NAFLD. Recently, MCJ, an inner mitochondrial membrane protein, has emerged as the first endogenous inhibitor of the electron transport chain complex I. In this project, we studied the role of MCJ in the pathogenesis of NAFLD and investigated the effect that the absence of MCJ exerts in the progression of the disease. Interestingly, we found that MCJ expression is increased during NAFLD. Moreover, MCJ silencing protected against hepatic lipid accumulation, liver injury and inflammation in the methionine-choline deficient mouse model of NASH. Apparently, loss of MCJ led to increased fatty acid β-oxidation, Krebs cycle function, and glycolysis rate, which maintained mitochondrial respiration and ATP production through oxidative phosphorylation. In other words, these metabolic adaptations were able to counteract the cytotoxic effects of fat accumulation on mitochondria and ultimately on hepatocytes. Altogether, MCJ arises as a key regulator of NAFLD paving the way for new promising therapeutic approaches.

2. INTRODUCTION

2.1. LIVER PATHOPHYSIOLOGY

The liver plays a central processing and distributing role in metabolism not only of carbohydrates, proteins and lipids, but also of hormones and drugs. Bile synthesis and immunity are other essential functions carried out by this organ.

Liver disease is an important cause of morbidity and mortality worldwide. In 2013, more than 30 million Americans had liver disease (American Liver Foundation, 2016) and 29 million people in the European Union (EU) suffered from a chronic liver condition (HEPAMAP EASL, 2016). Liver disease can be acute with fulminant liver failure or chronic and evolve over time to cirrhosis and liver cancer. Although liver disease is stereotypically linked to alcohol abuse or viral infections, bad dietary habits or excessive drug consumption have become new emerging risk factors.

2.2. NON-ALCOHOLIC FATTY LIVER DISEASE (NAFLD)

Non-alcoholic fatty liver disease (NAFLD) is the most common chronic liver disease in Western world, affecting 20-30% of the general population (Sattar *et al.*, 2014) and it is projected to be the leading indication for liver transplantation within a decade (Wong *et al.*, 2015). NAFLD is closely associated with obesity and features of the metabolic syndrome (hypertension, hyperlipidaemia, type 2 diabetes, and increased waist circumference), disorders with increasing prevalence worldwide (Brunt *et al.*, 2015).

NAFLD is a generic term that comprises a spectrum of clinical and histopathological disorders ranging from simple hepatic steatosis to a more complex pattern with inflammation (known as non-alcoholic steatohepatitis or NASH), fibrosis, cirrhosis and ultimately hepatocellular carcinoma (HCC), in the absence of alcohol intake. Although steatosis can be reversible, up to 44% of steatosis may progress to NASH (McPherson *et al.*, 2015), which is a significant risk factor for hepatic cirrhosis and HCC. According to the World Health Organization (WHO), in 2013, liver cirrhosis accounted for around 170,000 deaths in Europe and liver cancer accounted for around 47,000 deaths in the EU.

The "two-hit" model proposed by Day and James (1998) is currently the most accepted theory for NAFLD pathogenesis. According to this hypothesis, simple steatosis, as a result of insulin resistance and excessive fatty acid influx, constitutes the first hit. The first hit sensitises the liver to a second hit, which likely involves oxidative and endoplasmic reticulum (ER) stress, lipid peroxidation, and mitochondrial dysfunction. Thus, the second hit triggers hepatocyte damage and death, inflammation and fibrosis, and promotes disease progression from steatosis to NASH.

Hepatic steatosis or fat accumulation mainly in the form of triglycerides (TGs) in the cytoplasm of hepatocytes is the hallmark for NAFLD diagnosis. Dietary fats, circulating free fatty acids (FFAs) from lipolysis of adipose tissue, and *de novo* lipogenesis (DNL) are the main lipid sources of hepatocytes. Steatosis reflects a disordered homeostasis of lipid metabolism when lipid inputs exceed lipids utilized.

At the early stages of NAFLD, β-oxidation and very-low-density lipoprotein (VLDL) secretion are enhanced, possibly as a compensative mechanism in response to the overload of hepatic FFAs. β-oxidation in mitochondria provides energy (ATP) for the liver through the electron transport chain (ETC) and oxidative phosphorylation (OXPHOS). Due to electron leak in complexes I and III of the ETC, mitochondria become the major source of reactive oxygen species (ROS) production in cells. Thus, oxidative stress is produced in

hepatocytes as a result of an increased fatty acid oxidation (FAO). When β-oxidation and VLDL export are unable to utilize the overloaded FFAs, excessive FFAs will be esterified into TGs and stored in lipid droplets, resulting in hepatic steatosis.

Overproduction of ROS can lead to mitochondrial dysfunction. Impaired ATP homeostasis (Cortez-Pinto *et al.*, 1999) and defective ETC (Perez-Carreras *et al.*, 2003) are common indications of mitochondrial dysfunction and have been well documented in NAFLD.

Prolonged oxidative stress can activate the JNK pathway, which may trigger hepatocyte apoptosis. Moreover, high ROS levels can directly induce the transcription of proinflammatory cytokines (TNF-α, IL-6) through NFκB and activate the resident macrophages in the liver or Kupffer cells, which play a pivotal role in the inflammation during NASH by recruiting inflammatory cells (Baffy, 2009). Kupffer cells also help perpetuating liver injury by activating hepatic stellate cells (HSCs) through actions of several fibrogenic cytokines, especially TGF-β. HSCs are the key cells involved in fibrosis, which is a wound healing response characterized by an excessive deposition of collagen and other extracellular matrix (ECM) molecules resulting in formation of scar tissue and poor liver function.

Lifestyle modification focused on healthy eating, weight loss (when needed) and regular exercise or even bariatric surgery has been shown to revert hepatic steatosis. However, there is clearly a need for pharmacological therapy to treat the acute stages of NAFLD (Musso *et al.*, 2016).

2.3. METHYLATION-CONTROLLED J (MCJ) PROTEIN

MCJ, also known as DnaJC15, is a small protein (147 amino acids) member of the DnaJC subfamily of cochaperones. Unlike other DnaJ proteins, MCJ is not soluble since it contains a transmembrane domain. MCJ was first reported in human ovarian cancer cell lines, where *mcj* gene expression was found to be negatively regulated by methylation and correlated with increased chemoresistance (Shridhar *et al.*, 2001).

Hatle *et al.* (2013) identified the mouse ortholog of MCJ and showed that MCJ resides in the inner mitochondrial membrane of highly metabolic tissues (heart, liver and kidney) and immune cells. Within mitochondria, MCJ associates with and negatively regulates complex I of the ETC, becoming the first endogenous inhibitor. Importantly, Hatle *et al.* (2013) proved that MCJ deficiency leads to increased complex I activity, hyperpolarization of mitochondria, and increased generation of ATP, without affecting mitochondrial mass.

Normally, increased mitochondrial membrane potential (MMP) is associated with increased ROS due to the escape of electrons from transport chain. In contrast, the absence of MCJ enhanced complex I activity and accumulation of H^+ in the intermembrane space, but it did not increase ROS. In mammalian cells, especially hepatocytes and cardiomyocites, supercomplexes containing complexes I, III and IV have been characterized and defined as "respirasomes" (Acin-Perez *et al.,* 2008). The functions of the supercomplexes are likely to facilitate the transfer of electrons between complexes and to minimize the risk of releasing electrons that lead to ROS formation. It is therefore possible that the lack of MCJ facilitates the formation of supercomplexes, leading to overall increased complex I activity and MMP but no increase in ROS.

While under normal physiological conditions MCJ is dispensable, enhanced mitochondrial respiration in the absence of MCJ prevents the pathological accumulation of lipids in the liver under altered metabolic conditions, such as fasting and a high-cholesterol diet (Hatle *et al.,* 2013).

3. OBJECTIVES

Restoring the mitochondrial ETC activity in NAFLD could mitigate oxidative stress, which plays an important role in cell death, inflammation and fibrosis. Interestingly, MCJ has recently emerged as a novel endogenous inhibitor of ETC complex I. Taken together, the aim of this project is to study the role of the mitochondrial protein MCJ in the development of NAFLD and investigate the effect that the absence of MCJ exerts in the progression of the disease.

4. MATERIALS AND METHODS

Experimental procedures in animals were approved by the CIC bioGUNE Animal Care and Use Committee according to the criteria outlined in the "Guide for the Care and Use of Laboratory Animals" prepared by the National Academy of Sciences.

4.1. MCJ *IN VIVO* SILENCING OF MICE

Three-months-old male WT C57BL/6J mice (Jackson Laboratories) were fed a methionine (0.1%) and choline (0%) deficient diet (MCDD), an established model of NASH (Rinella *et al*., 2008). One week later, they were separated into two groups, each of which received twice (once a week) either 200 µl of a 0.75-µg/µl solution of MCJ-specific siRNA or

control siRNA using Invivofectamine® 3.0 Reagent (Thermo Fisher Scientific), through tail vein injection. Animals were sacrificed 4 weeks after the beginning of the diet.

4.2. HISTOLOGY

Paraffin-embedded sections of formalin-fixed liver samples were deparaffinised and rehydrated. Tissue sections were stained with haematoxylin and eosin (H&E), Sudan III, Sirius red, F4/80 antibody and periodic acid–Schiff (PAS) according to the CIC bioGUNE Histology Service routine procedures. Images were taken with a 20x objective from an Axio Imager A1 upright light microscope (Zeiss).

4.3. MITOCHONDRIA ISOLATION

Mitochondrial extracts from hepatic tissue were obtained using the Mitochondrial Fractionation Kit (ActiveMotif). Basically, lysis was performed in a pestle homogenizer using the gentle cytosolic buffer. The cellular lysate was subjected to several centrifugations to obtain crude mitochondria pellets.

4.4. PROTEIN ISOLATION AND WESTERN BLOTTING

After hepatic tissue homogenization (Precellys24, Bertin Instruments), addition of RIPA lysis buffer (protease inhibitor, sodium deoxycholate, 1 M NaF, 0.1 M ortovanadate) enabled total or mitochondrial fraction protein extraction. Protein was quantified by the BCA assay (Thermo Scientific) with a BSA standard curve. The extracted protein was separated by sodium dodecyl sulfate-polyacrylamide gel electrophoresis (SDS-PAGE) and transferred to nitrocellulose membranes or polyvinylidene difluoride (PVDF) membranes in the case of MCJ. The anti-mouse MCJ rabbit polyclonal antibody was generated as previously described by Hatle *et al*. (2013). JNK antibody is from Cell Signalling and JNK1/2 pT183/Y185 from Invitrogen. Apolipoprotein B antibody is from Chemicon International. As controls, GAPDH antibody (Abcam) or COXIV (Cell Signalling) were used. As secondary antibodies, anti-rabbit-IgG-HRP-linked (Cell Signalling), anti-mouse-IgG-HRP-linked (Santa Cruz Biotechnology) and anti-goat-IgG-HRP-linked (Santa Cruz Biotechnology) were used. Immunoreactive proteins were detected by Clarity ECL Substrate (BioRad), and exposed to X-ray films (Amersham) in a Curix 60 Developer (AGFA).

4.5. RNA ISOLATION AND QUANTITATIVE REVERSE TRANSCRIPTION POLYMERASE CHAIN REACTION (RT-qPCR)

Total RNA was extracted from frozen liver with TRIzol reagent (Invitrogen). RNA concentration and purity was determined using NanoDrop ND-1000 spectrophotometer (Thermo Scientific). 1-2 µg of total RNA was treated with DNAse (Invitrogen) and reverse transcribed into cDNA using M-MLV Reverse Transcriptase (Invitrogen) and random primers. Quantitative PCR was performed using SYBR® Select Master Mix (Applied Biosystems) and the ViiA7 Real-Time PCR System (Applied Biosystems). Primers were designed using the NCBI tool Primer-BLAST and provided by Sigma-Aldrich (**Supplementary Table 1**). The Ct values were extrapolated to a standard curve, and data was then normalized with the housekeeping expression (GAPDH).

4.6. MALATE DEHYDROGENASE 2 (MDH2) ACTIVITY ASSAY

Mitochondrial malate dehydrogenase (MDH2) activity was measured in mouse liver extracts using the Abcam Kit. The enzyme was inmunocaptured within the wells of the microplate and activity was determined by following the production of NADH. The generation of NADH is coupled to the 1:1 reduction of a reporter dye to yield a coloured reaction product whose concentration can be monitored by measuring the increase in absorbance at 450 nm.

4.7. RESPIRATION STUDIES IN ISOLATED LIVER MITOCHONDRIA

Liver mitochondrial respiration was measured at 37 °C by high-resolution respirometry using the Seahorse XF24-3 Extracellular Flux Analyzer (Agilent Technologies). For the measurement of the oxygen consumption rate (OCR), fresh liver mitochondria were isolated and plated in a XF24 cell culture microplate (Agilent Technologies), 5 µg per well. Mitochondria were incubated in a media containing substrates for both complexes I and II: glutamate (10 mM), malate (2 mM) and succinate (10 mM), in order to measure basal respiration. The instrument performed sequential compound addition and mixing while real time calculation of OCR. Firstly, ADP (4 mM) was added to asses "state 3" respiration, which is the actively respiring state. Then, the addition of ATP synthase inhibitor oligomycin (3 µM), allowed measurement of ATP-coupled oxygen consumption through OXPHOS. Carbonyl cyanide 4-trifluoromethoxy-phenylhydrazone (FCCP) (4 µM) is an uncoupling agent that allows maximum electron transport, and therefore measurement of proton leak. Finally, antimycin A (4 µM) and rotenone (2 µM), mitochondrial complex III and I inhibitors respectively, were performed to determine non-mitochondrial respiration.

The OCR values, expressed as pmol of O_2 per minute, were normalized with the total amount of protein quantified through the BCA method.

4.8. ATP LEVELS DETERMINATION

Intracellular ATP levels were determined *in vivo* and *in vitro* using the ATPlite luminescence assay system (PerkinElmer).

4.9. MCJ *IN VITRO* SILENCING OF PRIMARY MOUSE HEPATOCYTES

Hepatocytes were isolated from male C57BL/6J WT mice via collagenase perfusion. They were seeded at a density of 500,000 cells per collagen-coated culture well in fresh 10%-fetal bovine serum (FBS) minimum essential medium (MEM) (Gibco) supplemented with 1% penicillin, streptomycin and glutamine PSG (Invitrogen). In order to mimic NAFLD *in vitro*, primary hepatocytes were incubated overnight with 0% FBS MEM 1% PSG medium containing 400 μM oleic acid, and 1 μM rotenone (Sigma-Aldrich) was added 6 hours before cell harvesting. WT primary hepatocytes were transfected with 100 nM MCJ siRNA using Jetprime reagent (Polyplus). Controls were transfected with an unrelated siRNA (Qiagen).

4.10. BODIPY STAINING

Hepatocytes seeded in collagen-coated coverslips were incubated with BODIPY 493/503 (Molecular Probes) at a concentration of 10 μg/ml during 30 min. prior to fixation with 4% paraformaldehyde. DAPI (1 μg/ml) was added to the mounting medium. Images were taken with a 40x objective from an Axio Imager D1 fluorescence microscope (Zeiss). Quantification of lipid bodies was performed using Frida Software.

4.11. STATISTICAL ANALYSIS

Statistical significance was determined by two-way analysis of variance followed by a Student's *t* test using GraphPad Prism software.

5. RESULTS

5.1. MCJ EXPRESSION IS INCREASED IN NAFLD

Three-months-old WT C57BL/6 mice were fed for 4 weeks a MCDD, a well-established animal model of acute NAFLD. As in human disease (*data not shown*), MCDD-induced

NAFLD resulted in MCJ protein overexpression in mice (**Figure 1**). These data suggest a role for elevated levels of MCJ in the pathogenesis of NAFLD. We therefore wondered if MCJ silencing could benefit the understanding of the disease and the development of new drugs for its treatment.
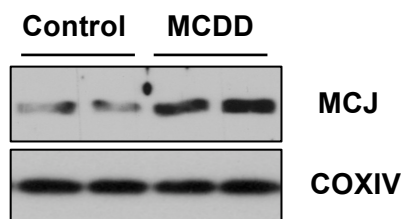

Figure 1. MCJ expression is regulated in NAFLD. Western blot analysis of MCJ expression in liver mitochondria of control and MCDD fed WT mice. MCJ protein was separated in a 15% (w/v) polyacrylamide gel. Complex IV (COXIV), a mitochondrial housekeeping, was resolved in a 11% (w/v) polyacrylamide gel.

5.2. MCJ SUPRESSION ATTENUATES MCDD-INDUCED LIVER INJURY

MCJ silencing was confirmed by Western blotting (**Figure 2A**). Western blot analysis showed that MCJ silencing was associated with insignificant JNK phosphorylation and therefore negligible triggering of apoptosis, compared to WT MCDD fed mice (**Figure 2B**). Importantly, mouse liver specimens provided by the CIC bioGUNE Histology Service revealed significantly reduced lipid content, fibrosis and inflammation in MCJ deficient animals (**Figure 2C**).
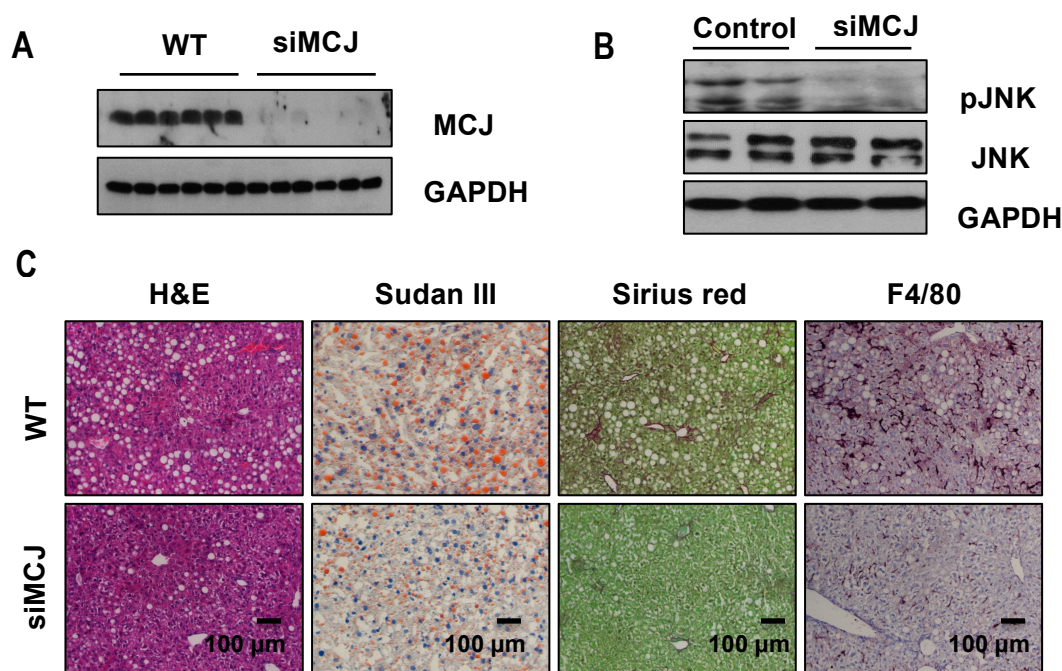

Figure 2. MCJ suppression attenuates MCDD-induced liver injury. (A) MCJ *in vivo* silencing confirmation by Western blotting in MCDD fed mice. MCJ protein and GAPDH, a cytosolic housekeeping, were resolved in a 15% (w/v) polyacrylamide gel. **(B) Western blot analysis of total JNK and pJNK expression measured in liver of WT**

and siMCJ MCDD fed mice. Proteins were resolved in a 11% (w/v) polyacrylamide gel. **(C) Liver injury analysis based on histological samples of WT and siMCJ MCDD fed mice.** Haematoxylin and eosin (H&E) stain is used for demonstration of cytoplasmic inclusions in pathological specimens. Sudan III enables detection of lipid accumulation within hepatocytes. Sirius red colours collagen fibres I and III and it is used to evaluate fibrosis levels. Anti-F4/80 antibody recognises a glycoprotein expressed by murine macrophages and it is used for inflammation assessment.

5.3. MCJ DEFICIENCY RESTORES FATTY ACID CATABOLISM IN THE LIVER

In NAFLD, hepatic fat accumulation could be mainly explained by: 1) enhanced fatty acid synthesis by DNL, 2) decreased VLDL export or 3) reduced capacity of β-oxidation. In order to determine the mechanism by which MCJ regulates hepatic lipid accumulation during NAFLD, we carried out the following assays.

Patricia Aspichueta´s group at the University of the Basque Country evaluated DNL by measuring the incorporation of [^{3}H]-acetate and reported no variations between siMCJ and control mouse livers (**Supplementary Figure 1**). Moreover, since VLDL secretion, measured as ApoB100 expression in serum, remained unaltered in both animal groups (**Figure 3A**), a regulation at the FAO level became our strong candidate.

Interestingly, PCR analysis revealed an overall increased gene expression in siMCJ MCDD fed mice of several proteins directly (CPT1, ACADM, ACADL, FATP2, ABCD1) and indirectly (PGC1α, NRF2) involved in FAO (**Figure 3B**). In other words, a reduced hepatic β-oxidation function driven by MCJ is thought to be the underlying cause of lipid accumulation during NAFLD.

Malate dehydrogenase enzymatic activity, which was used to evaluate the tricarboxylic acid (TCA) cycle activity, was significantly increased in siMCJ livers (**Figure 3C**). Consequently, the acetyl-CoA resulting from β-oxidation is meant to continue degradation into CO_2 in the TCA cycle and further energy production through the ETC and OXPHOS.

Liver mitochondrial respiration was evaluated by measurement of the OCR using Seahorse respirometry. siMCJ mouse livers showed significantly higher basal and "state 3" respiration than WT MCDD fed mice (**Figure 3D**). Moreover, ATP levels, which have been reported to be reduced during NAFLD, were significantly elevated in the absence of MCJ and comparable to control healthy animals (**Figure 3E**). These results are consistent with the previously described role of MCJ as a negative regulator of the ETC complex I under pathological conditions.
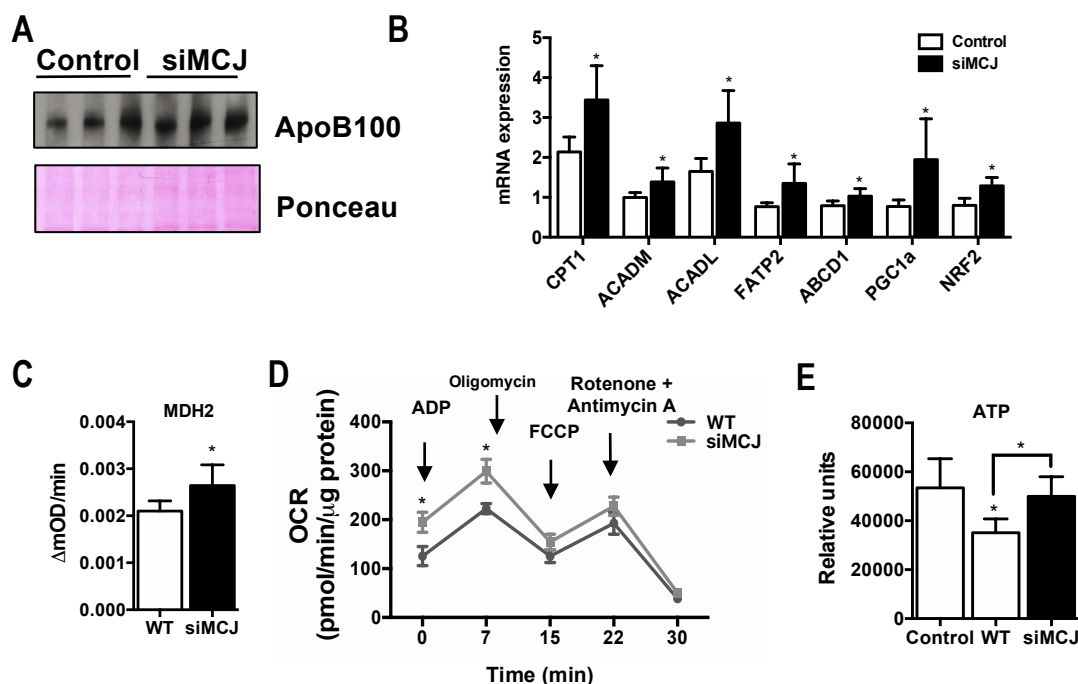
Figure 3. MCJ deficiency restores fatty acid catabolism in the liver. (A) Western blot analysis of ApoB100 expression measured in serum of WT and siMCJ MCDD fed mice. The protein was resolved in a 7% (w/v) polyacrylamide gel. Ponceau staining of nitrocellulose membranes was used as a loading control. **(B) mRNA expression analysis of FAO related genes measured in WT and siMCJ MCDD fed mice.** The tested genes encode for carnitine palmitoyltransferase 1 (CPT1), medium-chain acyl-CoA dehydrogenase (ACADM), long-chain acyl-CoA dehydrogenase (ACADL), fatty acid transport protein 2 (FATP2), ATP binding cassette subfamily D member 1 (ABCD1), peroxisome proliferator-activated receptor-gamma coactivator 1-alpha (PGC1a) and nuclear factor erythroid 2-related factor 2 (NRF2). Data was normalized to GAPDH housekeeping expression. **(C) Malate dehydrogenase 2 (MDH2) activity assay measured in liver extracts of WT and MCDD fed mice.** Enzymatic activity was expressed as product concentration (measured as the increase in absorbance at 450 nm) and divided by time. **(D) Seahorse analysis of ETC and OXPHOS activity measured in WT and siMCJ MCDD fed mice**. Liver mitochondria had been previously incubated in a media containing substrates for both complexes I and II to establish the OCR baseline. Then, the OCR was calculated while sequential addition of pharmacologic compounds: ADP, oligomycin, FCCP, and rotenone + antimycin A. **(E) Intracellular ATP production measured in liver of WT and siMCJ MCDD fed mice and compared with healthy control mice.** (*$p < 0.05$)

5.4. MCJ SILENCING INCREASES HEPATIC GLYCOLYSIS AND GLYCOGENESIS

Since the absence of MCJ leads to increased TCA cycle, mitochondrial ETC and ATP production through OXPHOS, we considered a regulation in the glycolytic pathway. PCR analysis proved that the genes involved in the first phase of the glycolysis (HK2, HK4, FBP1) and gluconeogenesis (PFKL), were overexpressed in siMCJ livers compared to controls (**Figure 4A**). Moreover, histological samples provided by the CIC bioGUNE Histology Service showed glycogen deposition in the liver of siMCJ MCDD fed mice (**Figure 4B**). These results suggest that the absence of MCJ also regulates carbohydrate metabolism to maintain mitochondrial function during NAFLD and to store excess energy.
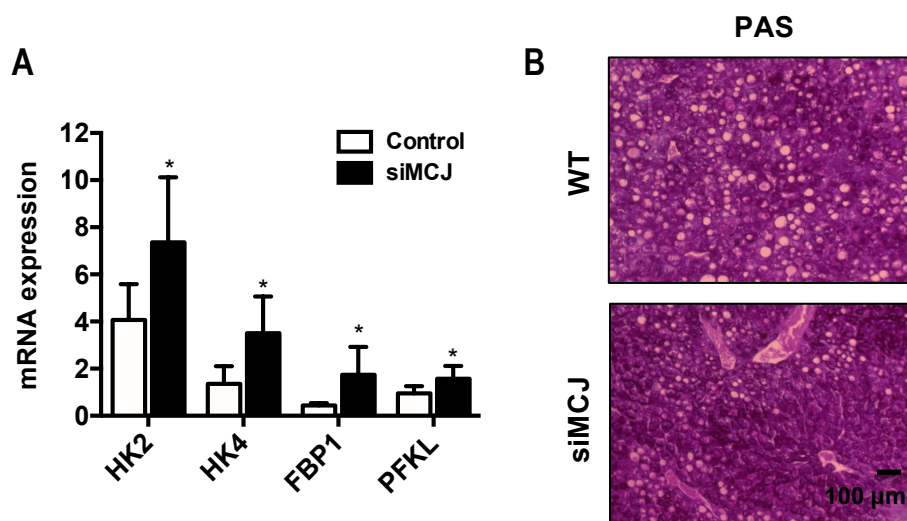
Figure 4. MCJ silencing increases hepatic glycolysis and glycogenesis. (A) mRNA expression analysis of glycolysis and glyconeogenesis genes measured in livers from WT and siMCJ MCDD fed mice. The tested genes encode for hexokinase 2 (HK2), glucokinase (HK4), fructose-bisphosphatase 1 (FBP1) and liver type phosphofructokinase (PFKL). Data was normalized with GAPDH housekeeping expression. (*p<0.05) **(B) Histology-based demonstration of glycogen storage in the liver of siMCJ MCDD fed mice through PAS staining.**

5.5. MCJ-DEPENDENT FATTY ACID CATABOLISM IS REGULATED BY ELECTRON TRANSPORT CHAIN COMPLEX I ACTIVITY

The above exposed results were verified *in vitro* by evaluating lipid bodies with BODIPY fluorescent staining (**Figures 5A and 5B**) and ATP production (**Figure 5C**) in isolated mouse primary hepatocytes. Accordingly, when treating hepatocytes with steatotic doses of oleic acid, MCJ silencing prevented cells from lipid accumulation and OXPHOS perturbation, in contrast with WT hepatocytes. However, the addition of rotenone, an exogenous ETC complex I inhibitor, reverted siMCJ hepatocytes to a pathological situation characterised by abundant lipid droplets and depletion of ATP intracellular levels. These results demonstrate that MCJ regulates β-oxidation and ATP production in the liver through complex I activity and could be useful for the treatment of NAFLD.
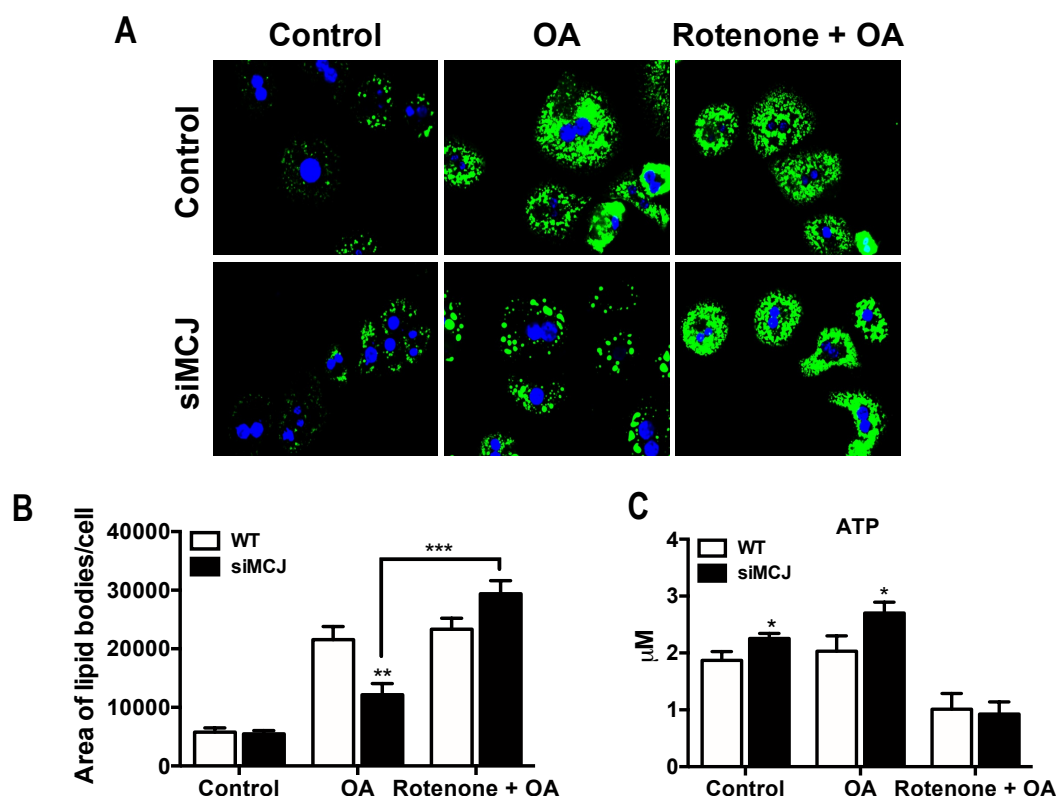
Figure 5. MCJ-dependent fatty acid catabolism is regulated by electron transport chain complex I activity. (A) BODIPY staining of lipid droplets in WT and siMCJ primary hepatocytes treated with steatotic doses of oleic acid (OA) in the absence and in presence of complex I inhibitor, rotenone. (**B**) **Lipid body quantification using Frida Software. (C) Intracellular ATP levels determination.** (*$p<0.05$, ** $p<0.01$, ***$p<0.001$)

6. DISCUSSION

Since mitochondrial protein MCJ is expressed during murine NASH but not in healthy animals (**Figure 1**), we considered silencing MCJ to further investigate the molecular mechanisms involved in the development of the disease. Thus, MCJ depletion revealed an increased activity of FA catabolism as mitochondrial β-oxidation (**Figure 3B**), TCA cycle (**Figure 3C**), ETC (**Figure 3D**) and OXPHOS (**Figure 3E**) were increased in MCDD fed mouse livers. Moreover, the glycolytic pathway was enhanced too (**Figure 4A**), possibly to feed the demands of an incredibly functional ETC. As a matter of fact, the accumulation of ATP and glycerol as a result of an increased lipid catabolism can be sensed by the liver as a signal to initiate gluconeogenesis to store the surplus energy in the form of glycogen (**Figure 4B**). We further verified *in vitro* that the enhancement of lipid oxidation was regulated by MCJ. Interestingly, addition of exogenous inhibitor of complex I rotenone to steatotic hepatocytes reverted the recovered situation driven by siMCJ back to pathological

(**Figure 5**). Surprisingly, despite an increased ETC activity, no ROS production was detected. Conversely, a reduction in apoptosis (**Figure 2B**), inflammation and fibrosis (**Figure 2C**) was observed, as Hatle *et al.* (2013) had also described before. Summing up, the liver specific deletion of the respiratory chain inhibitor MCJ attenuates the progression of NAFLD by enhancing β-oxidation.

Altogether, our final hypothesis of NAFLD pathogenesis is as follows. We suggest that inner mitochondrial membrane protein MCJ is able to bind and inhibit ETC complex I and the subsequent association of complex III to form supercomplexes. On the one hand, complex I inhibition may lead to a decreased mitochondrial respiration activity and OXPHOS. Moreover, the feeder pathways for ETC may be slowed down too. β-oxidation is directly linked to ETC through the TCA cycle. Thus, mitochondrial dysfunction, which is implicated in the pathogenesis of most liver diseases, might impair the oxidation of FAs leading to lipid accumulation within the liver, also known as hepatic steatosis (Day and James´s first hit). On the other hand, hampered supercomplex formation could lead to an inefficient transfer of electrons between complexes favouring electron leakage and subsequent ROS formation. Prolonged oxidative stress would trigger apoptosis, inflammation and fibrosis, and therefore exacerbate NAFLD progression to a more acute state (Day and James´s second hit) that could finally end in cirrhosis or even HCC.

7. CONCLUSION

The unravelling of NAFLD pathogenesis has led us to introduce MCJ as a druggable target that could help revert hepatic steatosis as well as NASH. Importantly, MCJ is detectable in the sera of NAFLD patients (*data not shown*), suggesting its value as a biomarker for the disease that would probably overcome the inconvenience of liver biopsy.

Additionally, parallel experiments conducted by Mª Luz Martinez-Chantar´s group have extended MCJ applications to drug induced liver injury (DILI) prevention and treatment, another major risk factor for acute liver failure nowadays. Several drugs, such as paracetamol, have been described to target mitochondrial dysfunction. It is possible that highly reactive paracetamol metabolites promote the interaction of MCJ with complex I, thereby interfering with formation of supercomplexes in the liver. Thus, the repression of MCJ expression seems to avoid hepatotoxicity by sustaining the formation of supercomplexes.

Fortunately, results from a number of on-going clinical trials have revealed that siRNA treatment is an efficient therapeutic approach to target genes in the liver (Wittrup and

Lieberman, 2015). Likewise, siRNA-targeting MCJ may also show efficacy for the treatment of NAFLD, DILI and presumably other liver disorders associated with mitochondrial dysfunction.

Finally, it is worth mentioning that MCJ suppression cannot always be considered as a beneficial approach. For example, low MCJ expression in breast cancer cells has proved to promote chemoresistance (Fernandez-Cabezudo *et al.*, 2016). Apparently, loss of MCJ expression could provide the necessary energy for cancer growth and ABC drug efflux transporters, which are highly dependent on mitochondria-derived ATP. In contrast with NAFLD and DILI therapeutic strategies, MCJ agonists could be used in combination with standard chemotherapeutic drugs to overcome chemoresistance, not only in primary cancers, but also in metastatic cancers that are highly refractory to any conventional therapies.

8. BIBLIOGRAPHY

Acin-Perez, R., Fernandez-Silva, P., Peleato, M.L., Perez-Martos, A., Enriquez, J.A. 2008. Respiratory active mitochondrial supercomplexes. Mol. Cell. 32:529 –539.

American Liver Foundation. The Liver Lowdown – Liver Disease: the big picture. Available from: http://www.liverfoundation.org/education/liverlowdown/ll1013/bigpicture. Last accessed: June 2017.

Baffy, G. 2009. Kupffer cells in non-alcoholic fatty liver disease: the emerging view. J. Hepatol. 51:212–223.

Brunt, E.M., Wong, V.W., Nobili, V., Day, C.P., Sookoian, S., Maher, J.J., Bugianesi, E., Sirlin, C.B., Neuschwander-Tetri, B.A., Rinella, M.E. 2015. Nonalcoholic fatty liver disease. Nat. Rev. Dis. Primers. 1:15080.

Cortez-Pinto, H., Chatham, J., Chacko, V.P., Arnold, C., Rashid, A., Diehl, A.M. 1999. Alterations in liver ATP homeostasis in human nonalcoholic steatohepatitis: a pilot study. JAMA. 282:1659–1664.

Day, C.P., James, O.F. 1998. Steatohepatitis: a tale of two ''hits''? Gastroenterology. 114:842–845.

Fernández-Cabezudo, M.J., Faour, I., Jones, K., Champagne, D.P., Jaloudi, M.A., Mohamed, Y. A., Bashir, G., Almarzooqi, S., Albawardi, A., Hashim, M.J., Roberts, T.S., El-Salhat, H., El-Taji, H., Kassis, A., O´Sullivan, D.E., Christensen, B.C., DeGregori, J.,

Al-Ramadi, B.K., Rincon, M. 2016. Deficiency of mitochondrial modulator MCJ promotes chemoresistance in breast cancer. JCI Insight. 1.

Hatle, K.M., Gummadidala, P., Navasa, N., Bernardo, E., Dodge, J., Silverstrim, B., Fortner, K., Brug, E., Suratt, B.T., Hammer, J., Radermacher, M., Taatjes, D.J., Thornton, T., Anguita, J., Rincon, M. 2013. MCJ/DnaJC15, an endogenous mitochondrial repressor of the respiratory chain that controls metabolic alterations. Mol. Cell. Biol. 33:2302-2314.

European Association for the Study of the Liver (EASL). HEPAMAP. A roadmap for hepatology research in Europe: An overview for policy makers. Available from: http://www.easl.eu/medias/EASLimg/News/3f9dd90221ef292_file.pdf. Last accessed: June 2017.

McPherson, S., Hardy, T., Henderson, E., Burt, A.D., Day, C.P., Anstee, Q.M. 2015. Evidence of NAFLD progression from steatosis to fibrosing-steatohepatitis using paired biopsies: implications for prognosis and clinical management. J. Hepatol. 62:1148–1155.

Musso, G., Cassader, M., Gambino, R. 2016. Non-alcoholic steatohepatitis: emerging molecular targets and therapeutic strategies. Nat. Rev. Drug Discov. 15:249–74.

Sattar, N., Forrest, E., Preiss, D. 2014. Non-alcoholic fatty liver disease. BMJ. 349:g4596.

Perez-Carreras, M., Del Hoyo, P., Martin, M.A., Rubio, J.C., Martin A., Castellano, G., Colina, F., Arenas, J., Solis-Herruzo, J.A. 2003. Defective hepatic mitochondrial respiratory chain in patients with nonalcoholic steatohepatitis. Hepatology. 38:999–1007.

Rinella, M.E., Elias, M.S., Smolak, R.R., Fu, T., Borensztajn, J., Green, R. M. 2008. Mechanisms of hepatic steatosis in mice fed a lipogenic methionine choline-deficient diet. J. Lipid Res. 49:1068–1076.

Shridhar, V., Bible, K.C., Staub, J., Avula, R., Lee, Y.K., Kalli, K., Huang, H., Hartmann, L.C., Kaufmann, S.H., Smith, D.I. 2001. Loss of expression of a new member of the DNAJ protein family confers resistance to chemotherapeutic agents used in the treatment of ovarian cancer. Cancer Res. 61:4258 – 4265.

Wittrup, A., Lieberman, J. 2015. Knocking down disease: a progress report on siRNA therapeutics. Nat. Rev. Genet. 16:543-52.

Wong, R.J., Aguilar, M., Cheung, R., Perumpail, R.B., Harrison, S.A., Younossi, Z.M., Ahmed, A. 2015. Nonalcoholic steatohepatitis is the second leading etiology of liver disease among adults awaiting liver transplantation in the United States. Gastroenterology. 148:547–555.

SUPPLEMENTARY DATA

Supplementary Table 1. Sequence of primers used for RT-qPCR.

Gene name	Symbol	Sequence
ATP Binding Cassette Subfamily D Member 1	ABCD1	Forward 5'-GACTCCGGAACAAACGTGAGG-3'
		Reverse 5'-CTTCATCTTGCCCTCGTCCA-3'
Acyl-CoA Dehydrogenase, Long Chain	ACADL	Forward 5'-GTCCGATTGCCAGCTAATGC-3'
		Reverse 5'-CACAGGCAGAAATCGCCAAC-3'
Acyl-CoA Dehydrogenase, Medium Chain	ACADM	Forward 5'-TCAAGATCGCAATGGGTGCT-3'
		Reverse 5'-GCTCCACTAGCAGCTTTCCA-3'
Carnitine Palmitoyltransferase 1	CPT1	Forward 5'-GACTCCGCTCGCTCATTCC-3'
		Reverse 5'-GAGATCGATGCCATCAGGGG-3'
Fatty Acid Transport Protein 2	FATP2	Forward 5'-CCGCAGAAACCAAATGACCG-3'
		Reverse 5'-TGCCTTCAGTGGATGCGTAG-3'
Fructose-Bisphosphatase 1	FBP1	Forward 5'-GTCTGTTTCGATCCCCTTGA-3'
		Reverse 5'-TCCAGCATGAAGCAGTTGAC-3'
Glyceraldehyde-3-phosphate dehydrogenase	GAPDH	Forward 5'-CGTCCCGTAGACAAAATGG-3'
		Reverse 5'-TTGATGGCAACAATCTCCAC-3'
Hexokinase 2	HK2	Forward 5'-GGGTAGCCACGGAGTACAAA-3'
		Reverse 5'-TGGATTGAAAGCCAACTTCC-3'
Hexokinase 4	HK4	Forward 5'-CTTTCCAGGCCACAAACATT-3'
		Reverse 5'-TGAGTGTTGAAGCTGCCA TC-3'
Nuclear Factor Erythroid 2-Related Factor 2	NRF2	Forward 5'-TGTAGGGTGGGGGTACAAAG-3'
		Reverse 5'-GAATCGGCGCTAAGGAACCC-3'
Phosphofructokinase, Liver Type	PFKL	Forward 5'-CATATATGTGGGGGCCAAAG-3'
		Reverse 5'-GACACACAGGTTGGTGATGC-3'

PPAR-gamma Coactivator 1 alpha	PGC1a	Forward 5'-AGACAGGTGCCTTCAGTTCAC-3'
		Reverse 5'-ACCAGAGCAGCACACTCTATG-3'
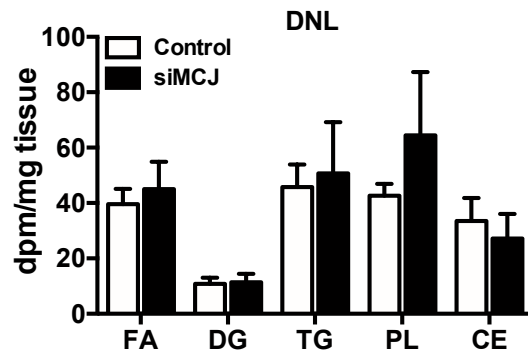
Supplementary Figure 1. DNL of fatty acids (FA), diglycerides (DG), triglycerides (TG), plasma phospholipids (PL) and cholesterol esters (CE) in livers from WT and siMCJ mice after the MCDD by measuring the incorporation of [³H]-acetate. Radioactivity was measured in a scintillation counter and expressed as disintegrations per minute (dpm).

ACKNOWLEDGEMENTS